QUATERNARY RESEARCH **48,** 267–279 (1997)
ARTICLE NO. QR971924

Implications of Late Pleistocene Glaciation of the Tibetan Plateau for Present-Day Uplift Rates and Gravity Anomalies

Georg Kaufmann and Kurt Lambeck

Research School of Earth Sciences, Australian National University, Canberra ACT 0200, Australia

Received January 29, 1997

Minimal and maximal models of Late Pleistocene Glaciation on the Tibetan Plateau are considered. The large ice sheet models indicate that disintegration of the ice sheet could have contributed up to 7 mm/yr of present vertical uplift and 2 mm/yr of horizontal extension. The former value can account for more than 50% of the observed uplift in central Tibet. The peak free-air gravity anomaly arising from the deglaciation would be around −5.4 mGal. In contrast, the smaller ice sheet models do not contribute significantly to the signals of present uplift and gravity anomalies. Modern geodetic measurements therefore have the potential to constrain the Late Pleistocene glaciation of the Tibetan Plateau. Assuming a large ice sheet over the Tibetan Plateau, the disintegration can contribute up to 6 m of eustatic sea-level rise.

Key Words: **glacial rebound; gravity anomalies; isostasy; Pleistocene glaciation; Tibet; uplift.**

INTRODUCTION

The Himalayan Range and the Tibetan Plateau cover an area of about 2×10^6 km^2, have an average elevation of 5 km, and include the highest mountains on Earth. The topography is a result of the continent–continent collision between India and Asia that started about 20 myr ago. In the last decades there has been considerable debate on the mechanisms forcing the present uplift of the entire area, ranging from *tectonic mechanisms* as a result of the ongoing continent–continent collision (see Harrison *et al.*, 1992, for a review) to *isostatic rebound* in response to enhanced erosion rates, especially during the Pleistocene ice ages and the related climatic changes, for example the weakening of the monsoon (Molnar and England, 1990; Burbank, 1992). It has also been argued (Kuhle, 1988b) that the present uplift rates of the Tibetan Plateau could be influenced by the melting of a large ice sheet covering the entire plateau at the last glacial maximum about 21,000 yr ago (LGM hereafter), resulting in glacial isostatic adjustment of the Tibetan Plateau during and after the deglaciation phase. Because of the large uncertainties in knowledge of the extent of the last glaciation of the Tibetan Plateau, the discussion of this contribution in the recent literature has been controversial.

In this paper, we investigate the effects of a glaciation of the Tibetan Plateau on present uplift rates and gravity anomalies using different space–time histories of the glaciated area during the last glaciation and the formulation for surface loading on a spherically symmetric, linear Maxwell-viscoelastic Earth. This method is commonly used to study effects related to the global mass redistributions during the Late Pleistocene glacial cycle (e.g., Nakada and Lambeck, 1987; Tushingham and Peltier, 1991; Johnston, 1993; Mitrovica *et al.*, 1994).

LATE PLEISTOCENE GLACIATION

The Tibetan Plateau embraces the major part of high Asia that also includes the mountain ranges of the Himalaya, the Karakoram, the Hindukush, and Pamir (Fig. 1). Today only 4% of this area is covered by glaciers (Derbyshire *et al.*, 1991); the vast majority of the Tibetan Plateau being dry and ice-free. Different estimates of the ice cover at the LGM can be found in the literature of the past decade, ranging from several individual ice caps, mainly centered over mountain ranges, and covering less than 13% of high Asia (Derbyshire *et al.*, 1991), to a regional ice sheet covering the entire plateau (Kuhle *et al.*, 1989; Gupta *et al.*, 1992b). These different hypotheses provide the basis for our ice models and will be discussed in detail.

First, we briefly review some of the earlier work concerning the ice sheet distribution on the Tibetan Plateau. More detailed descriptions can be found in Zheng (1989), Derbyshire *et al.* (1991), and Rutter (1995). Early in this century pioneering work was carried out by Sven Hedin during several expeditions in Asia. Hedin (1922) found no evidence for a large Late Pleistocene ice sheet over the Tibetan Plateau, arguing that the plateau was too dry to build up a substantial ice sheet. He recognized, however, that many of the present lakes are of glacial origin. From investigations on the east Pamir Plateau, Huntington (1906) had deduced the existence of an ice cap over this region as well as over northwestern

0033-5894/97 $25.00

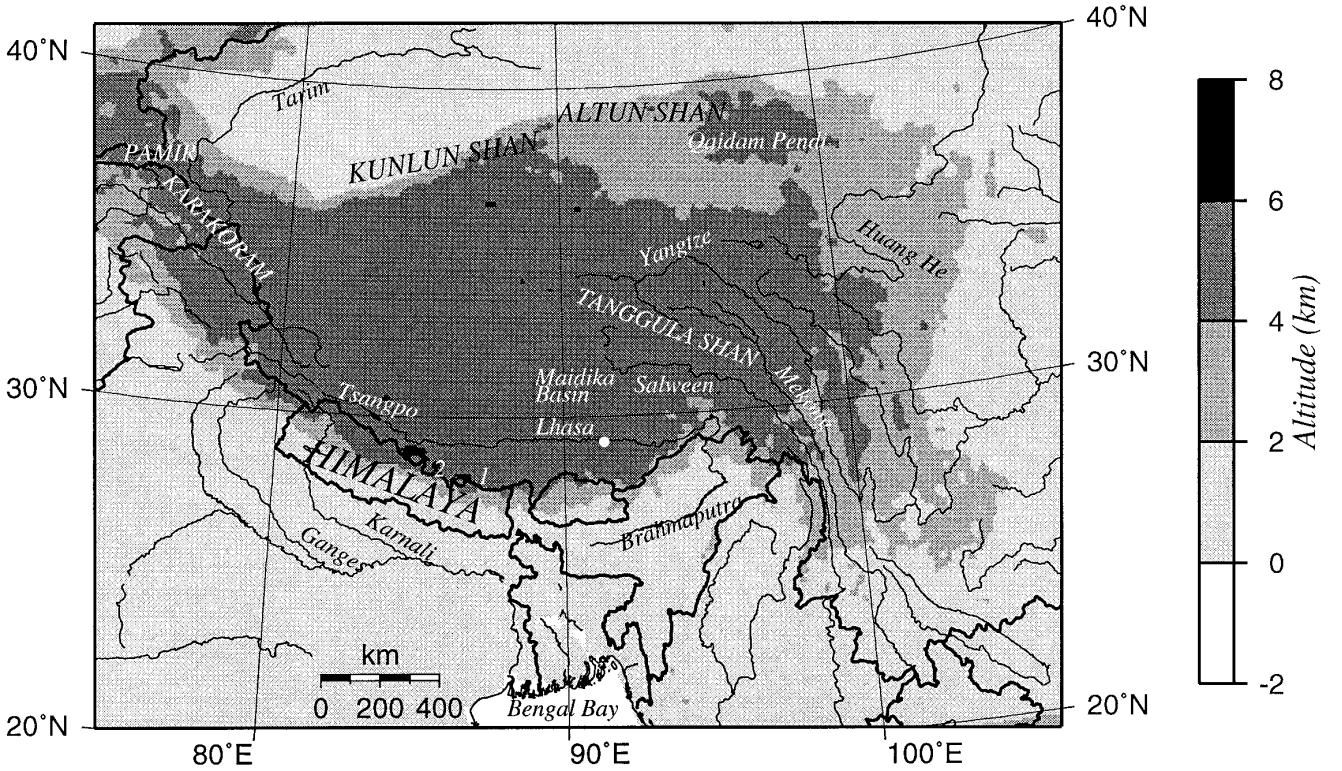

FIG. 1. Map of the Tibetan Plateau and surrounding mountain ranges. The filled circle indicates the location of Lhasa. The numbers refer to (1) Qomolangma Feng (Mt. Everest) and (2) Xixapangma Feng.

Tibet. Tafel (1908) proposed a large ice sheet covering the upper parts of the Huang He during the Late Pleistocene. Trinkler (1930) argued that the entire Tibetan Plateau was covered by a large ice sheet at the LGM. He drew this conclusion from a comparison of the glaciation of the Tibetan Plateau and the Pleistocene ice cover over New England. In contrast, Ward (1934) found no evidence for a single ice sheet and proposed only small ice caps over eastern Tibet, indicating regional differences in glaciation of the Tibetan Plateau. Renewed support for a large Late Pleistocene ice sheet was given by Sinitzin (1958), whereas von Wissmann (1959) argued for a glaciation that was restricted to mountain ranges, large glacier systems, and piedmont glaciers.

In a second phase of research, starting in the early 1960s, work was carried out more systematically by Chinese scientists. Luo and Yang (1963) proposed a flat-topped glacier over eastern Tibet but ongoing work by various groups pointed to an absence of geological evidence for a large ice sheet over the Tibetan Plateau. Only small ice caps were suggested, for example over northern Tibet (Wang and Zheng, 1965), with single ice caps not exceeding 500–1000 km^2 in size (Cui, 1964). However, more evidence for medium-sized ice caps was later found, for example an ice sheet over Maidika Basin (southeastern Tibet), which together covered around 3600 km^2 at the LGM (Zheng and Li, 1981). Sun and Wu (1986) mentioned glacial landforms around the Tibetan Plateau, which are ''widely spread'' and ''easily recognized,'' while Shi *et al.* (1986) came to the conclusion that there is no evidence for a large ice sheet over the Tibetan Plateau during the Late Pleistocene.

During the past decade the debate on the extent of the Pleistocene glaciation of the Tibetan Plateau during the LGM has continued to be controversial. The proposed models are based mainly on two points, geological observations in the region and the reconstruction of the glacier equilibrium line altitudes (ELA hereafter) that define the altitude of balance between glacial accumulation and ablation. Today the ELA ranges between 4500 and 6000 m across the mountain ranges of the Tibetan Plateau (Shi, 1992). The ELA is a function of the mean temperature, the radiation budget, and the precipitation in a specific area; thus, the existence of ice sheets strongly depends on these values.

Following Kuhle (1988a), the ELA at the LGM over the Tibetan Plateau was about 1200–1500 m lower than today, from which it is argued that a substantial ice sheet could have built up over the entire plateau during that time. Using additional geomorphological observations from western Tibet, Kuhle (1988c) proposed a large ice sheet with an average thickness of 1000–1200 m over the Tibetan Plateau. In the

central parts the ice thickness could have been as great as 2700 m or thicker than the present Greenland ice sheet. In a subsequent paper, Kuhle *et al.* (1989) modeled the rate of change in ice thickness using a three-dimensional snow balance model. These results supported their earlier hypothesis concerning complete ice cover over the Tibetan Plateau around the LGM, with ice thicknesses around 1000 m after 10,000 yr of snow accumulation and even greater thickness if longer accumulation times are assumed.

Gupta *et al.* (1992b), using δ^{18}O measurements from ice cores at Dunde ice cap (37°N, 96°E), derived a decrease in temperature of 4°–6°C at the LGM. According to the authors, this temperature estimate is in good agreement with other estimates on the Tibetan Plateau as well as estimates in other high mountain regions in the tropics. Based on this temperature decrease the authors derived a drop of the ELA close to the LGM of about 850 m. This supports reasonably well the values reported by Kuhle (1988c) and agrees with a lowering of ELA around 900–950 m observed in other high mountain regions (Rind and Peteet, 1985). Though the ELA at the LGM derived by Gupta *et al.* (1992b) allows the build up of a large ice sheet, the authors do not support the ice thickness estimates of Kuhle (1988c). Based on their calculations on oxygen isotopic mass balance between the Bengal Bay and the global oceans, the authors argue that an ice sheet of that size would have caused a regional negative δ^{18}O-decrease of about 1‰ in the Bengal Bay sediments relative to the global oceans between 10,000 and 8000 yr B.P. due to the meltwater brought in from deglaciation of the Tibetan Plateau. This assumes that the bulk of the runoff of the Tibetan ice sheet flowed through the Ganges River system. According to Gupta *et al.* (1992a), there is no evidence for such a decrease in Late Holocene times; instead, the authors favor an ice thickness of about 250 m at the LGM, based on calculations of the snow balance in the Tibetan Plateau.

In contrast to the areal extent of the LGM ice cover mentioned above, Derbyshire *et al.* (1991) derived an ice model for the Tibetan Plateau that is based mainly on geological evidence such as moraines and glacial striae. They conclude that the ice cover over the Tibetan Plateau at the LGM was greatest over northeastern and southern Tibet and that the ice cover is strongly related to the altitude and the morphology of the mountain ranges. The authors propose ice caps only over mountain ranges in addition to piedmont glaciers, for example, ice caps over Tanggula Shan, Kunlun Shan, the Karakoram, and Maidika Basin, resulting in less than 13% of the area being covered by ice. Consequently, Derbyshire *et al.* (1991) derived an ELA lowering at the LGM which was not uniform over the Tibetan Plateau, ranging from 1000 m on the southern slopes of the Himalaya to 500 m in the interior of the Tibetan Plateau and 300 m on the north slopes of Qomolangma Feng and Xixapangma Feng.

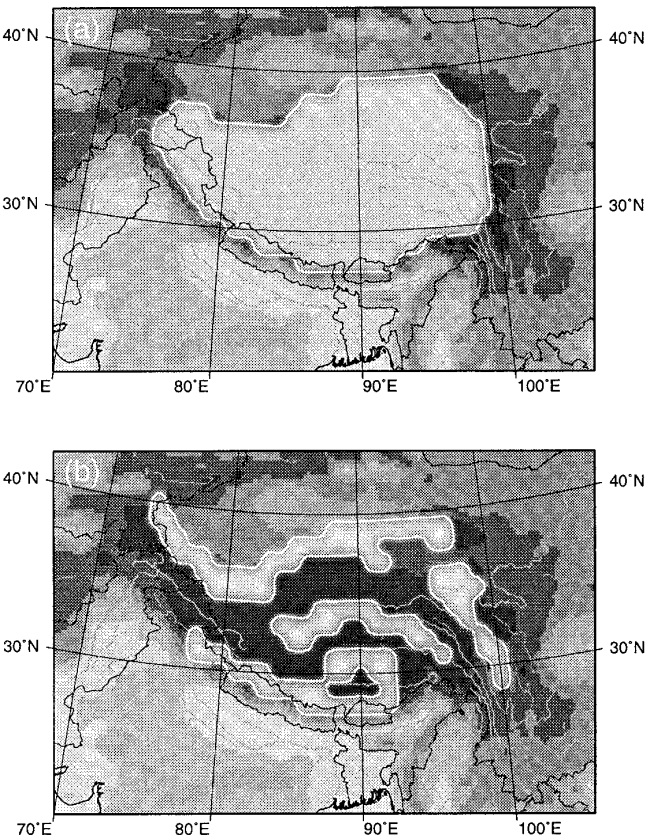

FIG. 2. Areal extent of ice models KUHLE and GUPTA (a) and DERBY (b) at the LGM.

Based on the controversial ice sheets proposed for the Tibetan Plateau by Kuhle *et al.* (1989), Gupta *et al.* (1992b), and Derbyshire *et al.* (1991), we have derived four different ice models for high Asia. The areal extent of the ice models KUHLE and GUPTA at the LGM is illustrated in Figure 2a. The ice limits of the two models are the same and encompass the entire Tibetan Plateau. The maximum ice thickness for the two models is 1000 and 250 m, respectively. The areal extent of ice model DERBY at the LGM is much more restricted (Fig. 2b), with the ice confined to mountains and piedmont glaciers. The maximum ice thickness is assumed to be 250 m. Due to the lack of information concerning the glaciation history, we have used a linear growth phase for these ice models, starting at about 105,000 yr B.P. and reaching the maximum ice thickness at the LGM about 22,000–21,000 yr B.P. The deglaciation, which is assumed to be linear, ended about 8000 yr B.P. This glaciation cycle is a first-order approximation of the glaciation histories used to model the space–time history of the global Pleistocene ice sheets (e.g., Mitrovica and Davis, 1995; Kaufmann, 1997) and adequate to give order-of-magnitude estimates of the rebound.

For the fourth ice model, TIBET-4, the entire Tibetan

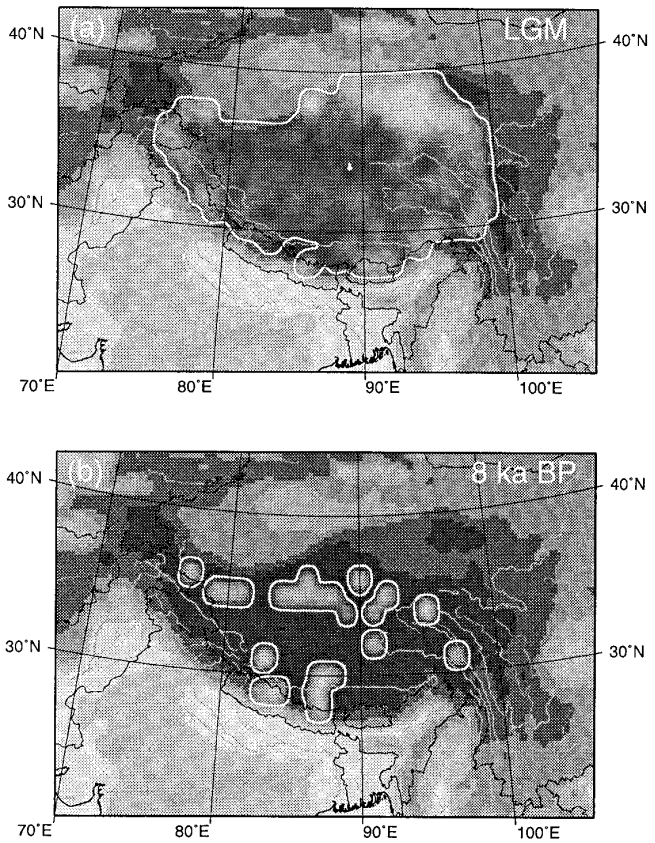

FIG. 3. Space–time history for two selected epochs of the ice model TIBET-4.

Plateau is covered by ice up to an altitude of 6000 m, consistent with the geomorphological observations reported by Kuhle *et al.* (1989). These authors mentioned the different shape of mountain ranges, with mountains above 6000 m sharply peaked, but smoothly shaped peaks below this altitude, showing glaciogenic influences. We note that the relation of these glaciogenic features to the Late Pleistocene glaciation phase is not clearly *a priori.* Thus, the determination of exposure ages across the different morphogenic areas is essential to constrain the glaciation over the Tibetan Plateau. We regard the ice model TIBET-4 as a maximalistic model for the glaciation at the LGM.

This fourth ice model is illustrated in Figure 3 for two different epochs. At the LGM, the plateau is assumed to have been covered by an ice sheet with a minimal thickness of about 1000 m over the central and western parts of the area, increasing towards 1500 m over the river catchments in the eastern plateau, and with an ice dome reaching more than 3000 m thickness over Qaidam Pendi. The deglaciation history for TIBET-4 is closely related to the increase of the ELA according to Gupta *et al.* (1992b), such that the area starts becoming ice-free in lower regions of the Tibetan Plateau as the ice retreats toward the higher mountain ridges. Shortly after 8000 yr B.P. the last ice in the model has melted completely.

UPLIFT HISTORIES

Since the beginning of the collision of India and Asia about 20 myr ago (e.g., Harrison *et al.*, 1992) the area of the Himalaya and the Tibetan Plateau has experienced uplift and erosion, although it remains uncertain whether or not the net uplift, given by the difference of uplift rate and erosion rate, was uniform. Several estimates on uplift rates have been published, ranging from a *linear* uplift of around 3–4 mm/yr for the NW Karakoram (Schneider, 1957, pp. 468 and 475), a *nonlinear* uplift of the Himalaya with uplift rates of less than 1 mm/yr before the Quaternary and up to 5 mm/yr during the Quaternary (Zeitler, 1985, empirical relation derived from isotopic dating in northern Pakistan), and an *episodic* uplift for the Himalaya with two phases of enhanced uplift rates of up to 5 mm/yr between 10.9 and 7.5 myr ago and from 0.9 myr on (Copeland and Harrison, 1990; Amano and Taira, 1992, derived from sedimentary deposits in Bengal Bay). Additionally, Molnar (1987) estimated uplift rates of about 5 mm/yr for the Himalaya from deformation of river terraces in the Nepal Himalaya, and Kuhle (1988b) quotes uplift rates of about 10–15 mm/yr as an integral value for Tibet and the Himalaya, but only 4–8 mm/yr for the Himalaya alone. Recently, Jackson and Bilham (1994) reviewed leveling data from Nepal and Tibet to constrain the deformation of the Himalaya. The two leveling lines were considered to have a poor signal-to-noise ratio and were thus regarded as only of limited use in inferring long-wavelength uplift rates of the Himalaya, relative to the surrounding regions, of 6.2 ± 10 and 7.5 ± 5.6 mm/yr for the two lines.

The above-mentioned uplift rates in the mountain ranges can be attributed mainly to tectonic forces in the Himalaya and the Karakoram. Comparing these values with observed present uplift rates greater than 10 mm/yr given on a Chinese tectonic map (1987) for the central Tibetan Plateau (reported by Kuhle, 1988b), the observed value exceeds the tectonically based uplift estimates by about two to three times. This raises the question whether there are other, nontectonic, contributions to the present uplift rates of the Tibetan Plateau, for example a component resulting from the ongoing glacial isostatic adjustment due to the melting of the Pleistocene ice cover of the Tibetan Plateau.

INTERPRETATION

The response of the Earth to surface loading, such as large ice sheets, mountain ranges, volcanoes, and sedimentary deposits is a classical problem in geophysics. For time scales characteristic of glacial cycles, the Earth is often modeled as a linear Maxwell-viscoelastic continuum, thus accounting

both for the instantaneous elastic response and the time-dependent viscous flow. The problem is then solved for an earth model divided into several layers, in which the physical properties of the Earth are supposed to represent average earth mantle values. Several numerical methods have been employed to solve the governing mechanical and gravitational field equations. We have adopted the normal mode approach (Love, 1911; Longman, 1962; Peltier, 1974) to describe the response of the Earth to an applied surface load in terms of Love numbers and a pseudospectral approach introduced by Mitrovica and Peltier (1989) to calculate three-dimensional deformations of the Earth to surface loading. Extensive tests have shown that the results are consistent with those obtained by Nakada and Lambeck (1987) and Johnston (1993) when the same assumptions are made about the Earth's physical properties.

Predictions of uplift rates, gravity anomalies, and other observable parameters related to the deformation induced by surface loads are strongly dependent on the rheology of the Earth's mantle. Thus, once the ice sheet distribution is known, it is possible to determine the rheological properties of the Earth's mantle. In fact, this approach is widely used in studies of postglacial land uplift (e.g., Tushingham and Peltier, 1991; Lambeck *et al.,* 1996) to determine both the thickness of the elastic lithosphere and the viscosity profile in the Earth's mantle. On the other hand, assuming that the properties of the Earth are known, theoretical predictions can be used to improve the space–time history of a poorly constrained ice sheet (e.g., Lambeck, 1996). In view of the wide range of ice models proposed for the Late Pleistocene glaciation of the Tibetan Plateau, we will assume that the properties of the Earth's mantle are known *a priori.* Using inferences from both interpretations of postglacial land uplift (e.g., Lambeck *et al.,* 1996; Mitrovica, 1996) and long-wavelength geoid signals (e.g., Richards and Hager, 1984), we define three earth models with upper and lower mantle viscosities (in Pa sec) of $10^{21}/2 \times 10^{21}$ (A), $7 \times 10^{20}/7 \times 10^{21}$ (B), and $4 \times 10^{20}/10^{22}$ (C), thus primarily reflecting the uncertainties in the increase of mantle viscosity across the 670-km seismic discontinuity. The thickness of the elastic lithosphere for all three models is 70 km. Additionally, we vary the latter value for earth model B, using thicknesses of 30 km (B′) and 120 km (B″), respectively. All earth models represent compressible Maxwell-viscoelastic rheologies and the elastic properties are derived from the seismic model PREM (Dziewonski and Anderson, 1981). The Earth's core is treated as an inviscid fluid.

In the next three sections we focus our interest mainly on the predictions based on earth model B, which represents a generally accepted viscosity profile for the upper 1800 km of the earth's mantle derived from postglacial rebound (e.g., Lambeck *et al.,* 1990; Mitrovica, 1996). Results derived from the other earth models will only be discussed briefly because our calculations show that the inferences about present observable parameters are primarily influenced by the space–time history of the ice model and are less dependent on the earth model considered in this study.

GLACIAL ISOSTATIC UPLIFT RATES

A glaciation cycle of about 100,000 yr will result in deformation of the Earth's lithosphere and mantle, the amplitude of which strongly depends on the mass of the ice sheets growing and melting during that period. Therefore, we expect large differences in the present uplift rates arising from the melting of the different ice models discussed above, which we have chosen to cover the entire range of plausible ice models, from the minimalistic model DERBY to a maximalistic ice cover described by model KUHLE.

In Figure 4 we have plotted present radial and tangential velocities for ice model KUHLE. Here the radial velocities indicate movements perpendicular to the (spherical) surface of the Earth, while tangential velocities describe movements parallel to the Earth's surface. We observe that the radial uplift pattern closely follows the shape of the ice model, with radial uplift rates ranging from 1 mm/yr around the former ice margin toward 3–4 mm/yr in the center of the formerly glaciated region. The entire Tibetan Plateau experiences uplift rates above 2 mm/yr. This updoming of the area glaciated during the Late Pleistocene is a characteristic feature also observed in formerly ice-covered regions of Northern America and Scandinavia (e.g., Ekman, 1996), and it can be related to the glacial isostatic adjustment in these areas. Comparing the maximum value of 3.9 mm/yr (Table 1) with uplift rates of up to 10 mm/yr in Scandinavia (Ekman, 1996) and 5 mm/yr in the Barents Sea (Kaufmann, 1997), we find that the effects of a glaciation on the Tibetan Plateau according to the extensive ice cover proposed by Kuhle (1988b) are comparable to effects in the Northern Hemisphere in the centers of Late Pleistocene glaciation. The uplift pattern in Figure 4 is surrounded by an area of subsidence of about −1 mm/yr, resulting from the collapse of the forebulge related to the former ice sheet.

Next we discuss the tangential velocity field imposed by the deglaciation process. Ice model KUHLE leads to the prediction of significant horizontal movements within the formerly glaciated area, inducing flowlines that form a pattern radially flowing away from the central Tibetan Plateau. The largest tangential velocities (1.0 mm/yr) occur across the former ice sheet margin, which coincides with the mountain ridges surrounding the plateau (Fig. 1). Thus, a large ice cover over the area would result in a glacially induced extension of the Tibetan Plateau of around 2 mm/yr. Outside the Tibetan Plateau, the present tangential velocity field is oriented outward from the center of the formerly glaciated area. However, both the magnitude and the direction of the

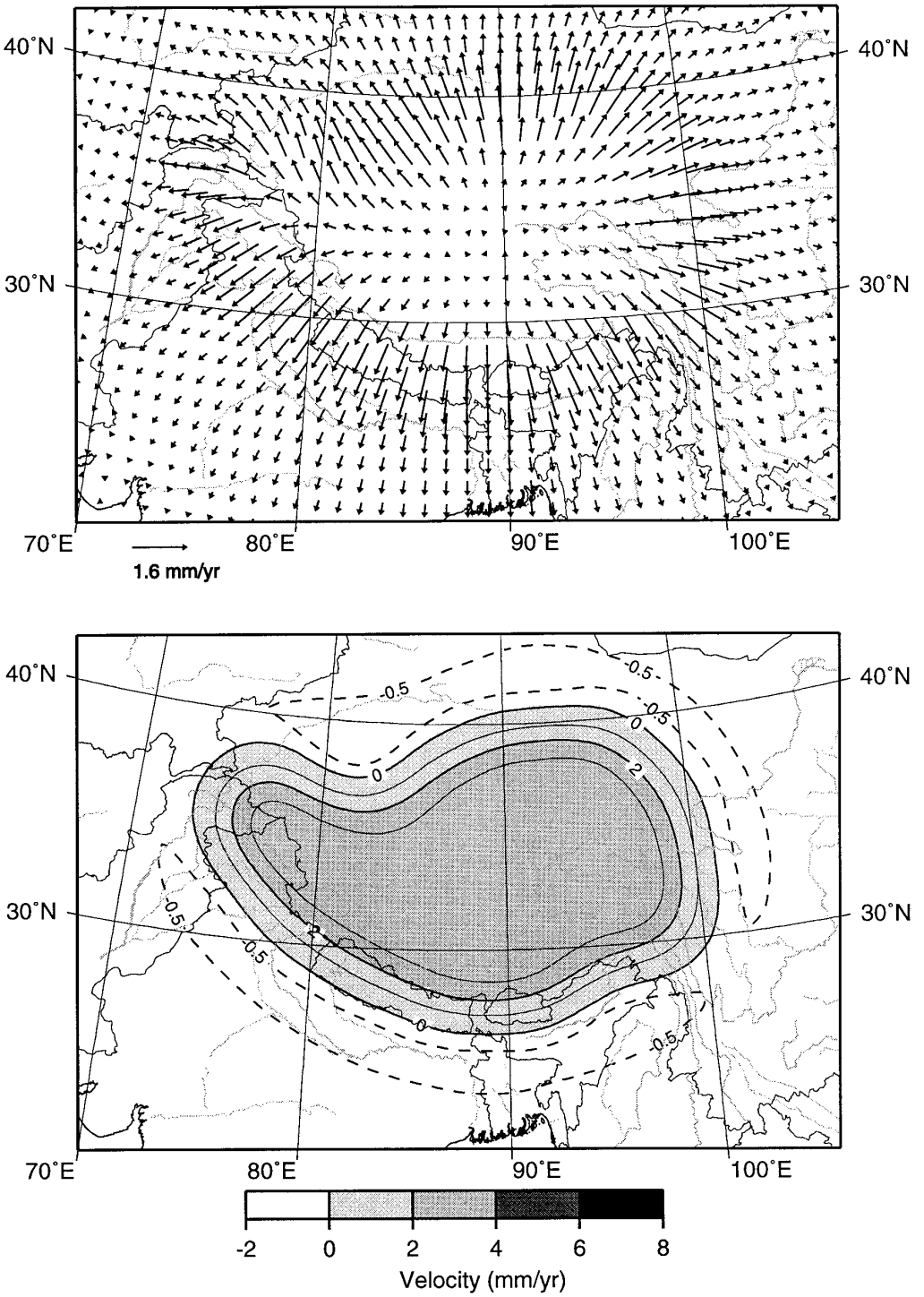

FIG. 4. Present tangential (top) and radial (bottom) velocities over high Asia according to ice model KUHLE.

tangential velocity field outside the formerly glaciated area are a strong function of the earth model, such that an earth model that is less viscous in the upper mantle would result in inward flow (not shown). Therefore, an interpretation of the horizontal velocity field outside the Tibetan Plateau will be strongly biased by the particular earth model used.

The predicted present radial uplift rates are also a function of the earth model, particularly for TIBET-4 (Table 1). Thus,

TABLE 1
Maximum Present Radial Uplift Rates (in mm/yr) for Different Ice and Earth Models

Ice model	A	B	C	B′	B″
KUHLE	3.7	3.9	2.8	4.6	4.0
GUPTA	0.9	1.0	0.7	1.2	1.0
DERBY	0.5	0.6	0.4	1.1	0.5
TIBET-4	8.0	7.5	3.8	11.5	4.8

the maximum values for the uplift tend to decrease with decreasing upper mantle viscosity or with increasing lower mantle viscosity, although the dependence on the latter is not very strong because the wavelength of the ice model is relatively short. Lower values for the upper mantle viscosity lead to a more rapid relaxation and hence to lower present uplift rates. For ice model KUHLE, the predicted uplift rates for an upper mantle viscosity of 10^{20} Pa sec are less than 1 mm/yr, a rate that would be difficult to detect by present geodetic measurements. A variation of lithospheric thickness investigated using earth models B′ and B″ results in a large increase in uplift rate relative to earth model B, if the lithospheric thickness is reduced, but a similar uplift rate, if the lithospheric thickness is increased.

The ice model GUPTA is identical to ice model KUHLE, except that the ice thickness is reduced. According to the linear relation between ice thickness and displacement in the theoretical model used, we can simply rescale the results from ice model KUHLE using a factor of 0.25 arising from the relation between the ice thicknesses in both ice models. Both the radial and tangential velocity patterns in Figure 4 remain valid for ice model GUPTA. Thus, we find that the maximum radial uplift rate is reduced to 1 mm/yr (Table 1) and the tangential velocities become insignificantly small. Comparing the different radial uplift rates for ice model GUPTA in Table 1, we find that the differences arising from the rheological properties of the earth models considered are only minor. Therefore we conclude that a Pleistocene glaciation of the Tibetan Plateau as proposed by Gupta *et al.* (1992a) does not significantly contribute to present uplift rates.

In Figure 5 we have plotted present radial and tangential velocities for ice model DERBY. As a consequence of the limited extension of the glaciated area we find a modified radial uplift pattern with a maximum radial uplift rate about 0.6 mm/yr around the Lhasa region. The tangential velocity field reflects the areal extent of the ice caps in ice model DERBY, with flowlines pointing outward from previously glaciated areas, for example Maidika Basin, Kunlun Shan, and Altun Shan. However, the maximum tangential velocities do not exceed 0.15 mm/yr and are therefore negligible. Again we find only minor differences in the radial uplift rate for the different earth models (Table 1). We can conclude that the limited Pleistocene glaciation of the Tibetan Plateau proposed by Derbyshire *et al.* (1991) makes no significant contribution to present uplift rates.

In ice model TIBET-4 the maximum ice thickness is located over Qaidam Pendi. Consequently, the maximum present uplift rates can be observed over this area, exceeding 7 mm/yr (Fig. 6, Table 1). In contrast to ice model KUHLE, the uplift rates above 2 mm/yr are now more focused on the eastern part of the Tibetan Plateau. The pattern of the tangential velocity field also reflects the enhanced horizontal movement of the eastern plateau, with tangential velocities about 1 mm/yr radially directed away from Qaidam Pendi. Thus, horizontal movements across the Himalayan range are reduced relative to ice model KUHLE. We expect a glacially induced stress field with extension mainly around Qaidam Pendi and extension rates about 2 mm/yr.

In Figure 7 we have plotted present radial velocities for ice models KUHLE, DERBY, and TIBET-4 along two profiles across the Tibetan Plateau. For the W–E profile (Fig. 7a), we find that both maximum ice models KUHLE and TIBET-4 reach maximum uplift rates over the eastern part of the profile. Of greater interest is the greater spatial variability in uplift rates along the profile for ice model TIBET-4, for which the uplift rates are concentrated over eastern Tibet as a result of the large ice cover over Qaidam Pendi. The uplift rate resulting from ice model KUHLE is much smoother across the profile, resulting in uplift rates of over 2 mm/yr across the entire Tibetan Plateau, as already mentioned. Finally, we observe uplift rates of less than 0.6 mm/yr for ice model DERBY, which are negligible relative to the tectonic contribution.

The predictions for the S–N profile (Fig. 7b) essentially confirm the results obtained along the W–E profile. We observe a large updoming of the Tibetan Plateau for ice model KUHLE and a shift of the area around the maximum uplift rates toward the northern end of the profile for ice model TIBET-4. Again, ice model DERBY has an insignificantly small contribution to the present uplift rate.

EUSTATIC SEA-LEVEL RISE

The melting of an ice sheet covering the entire Tibetan Plateau during the LGM would have contributed a large amount of meltwater to the oceans. On a more global scale, the meltwater from the Tibetan Plateau can contribute a significant amount to the total eustatic sea-level rise (ESL) resulting from the melting of the large Pleistocene ice sheets and the thermal expansion of the oceans following the global climatic warming. Following Fairbanks (1989), who dated corals from Barbados in the Caribbean Sea, the total ESL rise between the LGM and today is close to 130 m. When we compare this observed value with predicted contributions arising from melting of major

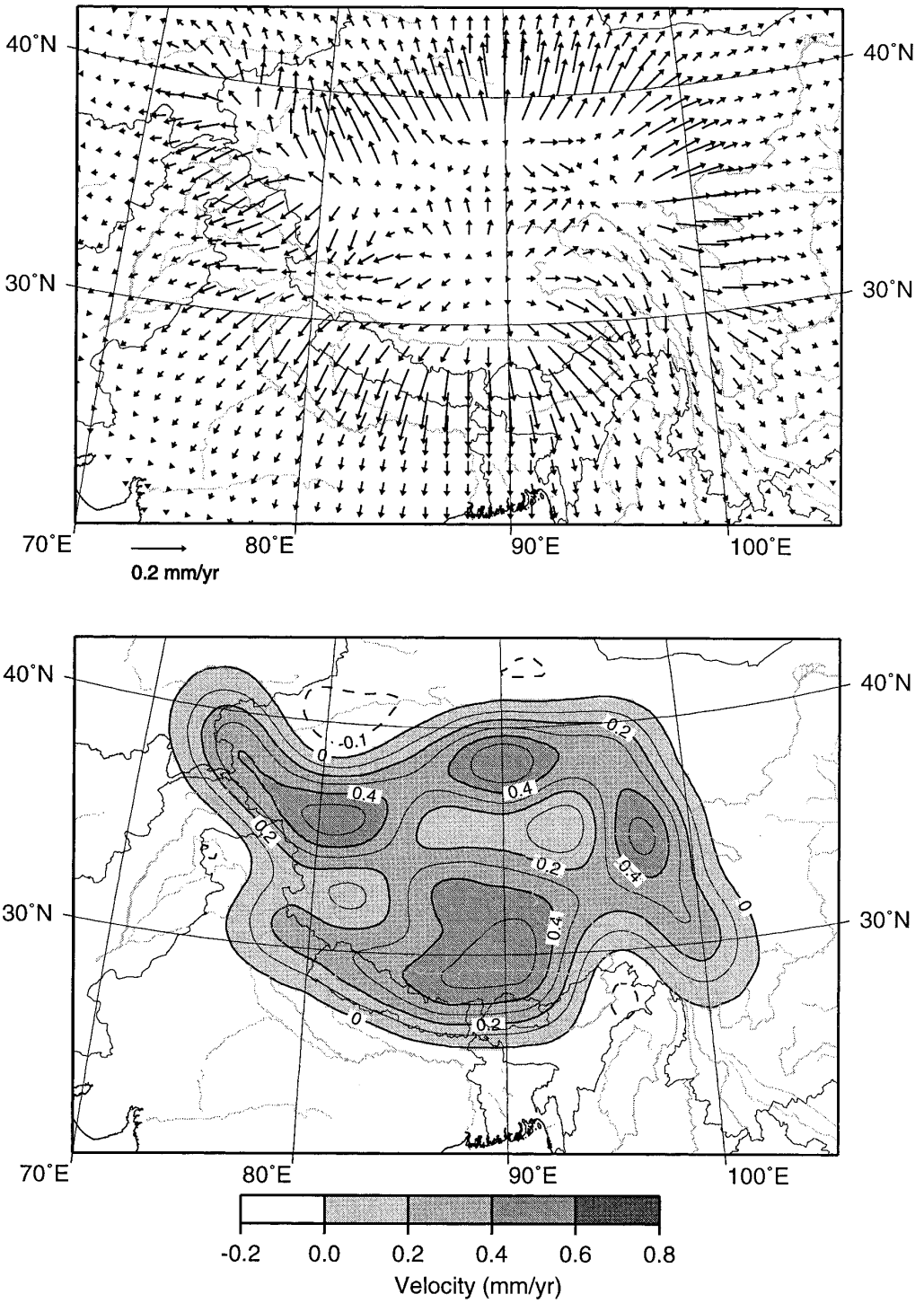

FIG. 5. Present tangential (top) and radial (bottom) velocities over high Asia according to ice model DERBY.

Pleistocene ice sheets in the northern hemisphere at about 83–89 m (e.g., Denton and Hughes, 1981; Peltier, 1994) and Antarctica at about 12–37 m (e.g., Nakada and Lambeck, 1988; Huybrechts, 1992), we find predictions for the total ESL rise ranging from 95 to 126 m, with its largest uncertainties coming from the Antarctic contribution.

Following the arguments for a Pleistocene glaciation of the Tibetan Plateau summarized in this paper, we can bound

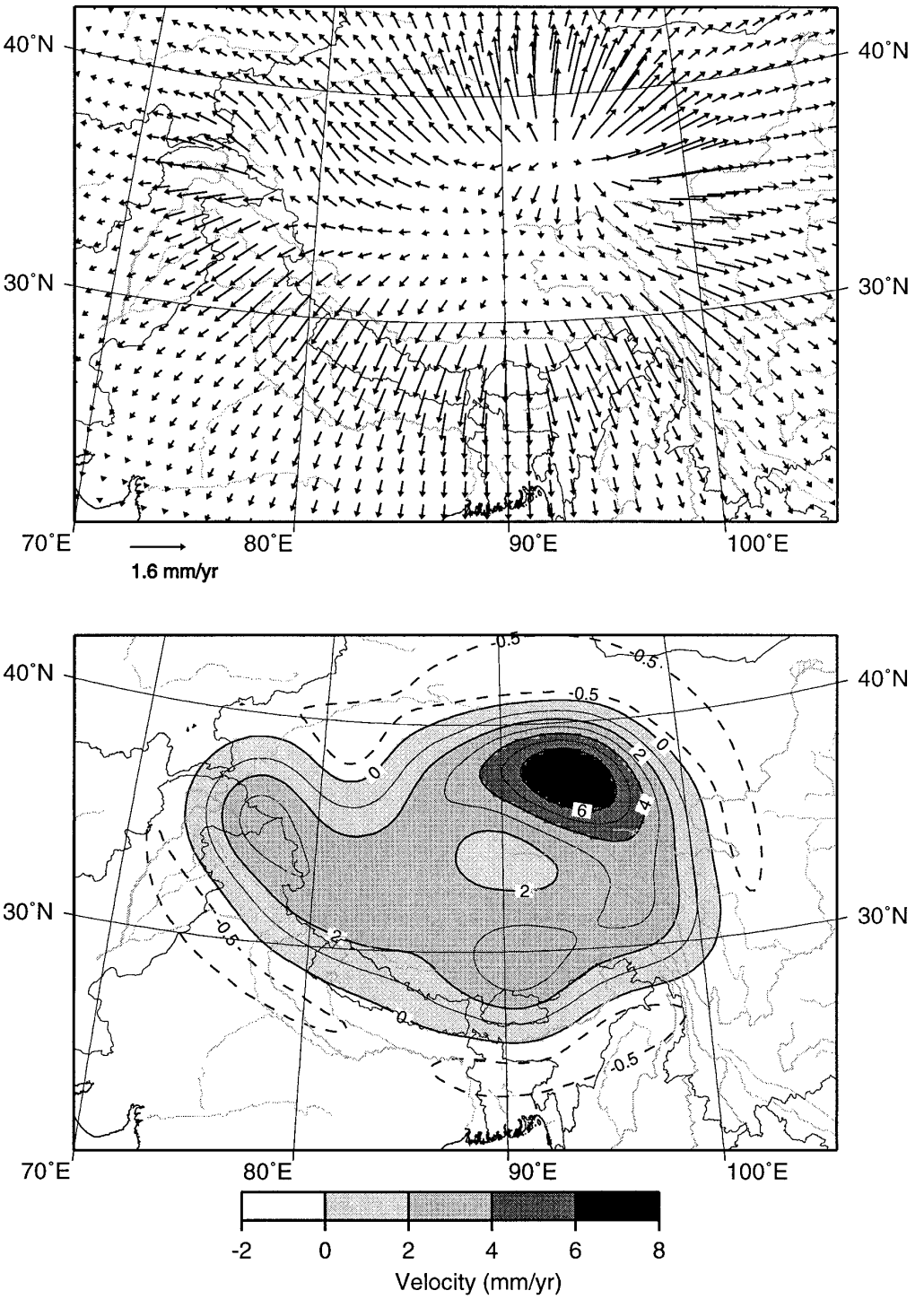

FIG. 6. Present tangential (top) and radial (bottom) velocities over high Asia according to ice model TIBET-4.

one more possible ESL contribution using predictions for the ice models adopted in this approach. For this purpose we have plotted the eustatic sea-level rise related to the melting of a Tibetan ice sheet in Figure 8 for ice models KUHLE, DERBY, and TIBET-4, and additionally we have summarized the ESL contribution at the LGM in Table 2. For a complete ice cover at the LGM, the contribution to eustatic sea-level rise can be more than 5 m for ice models

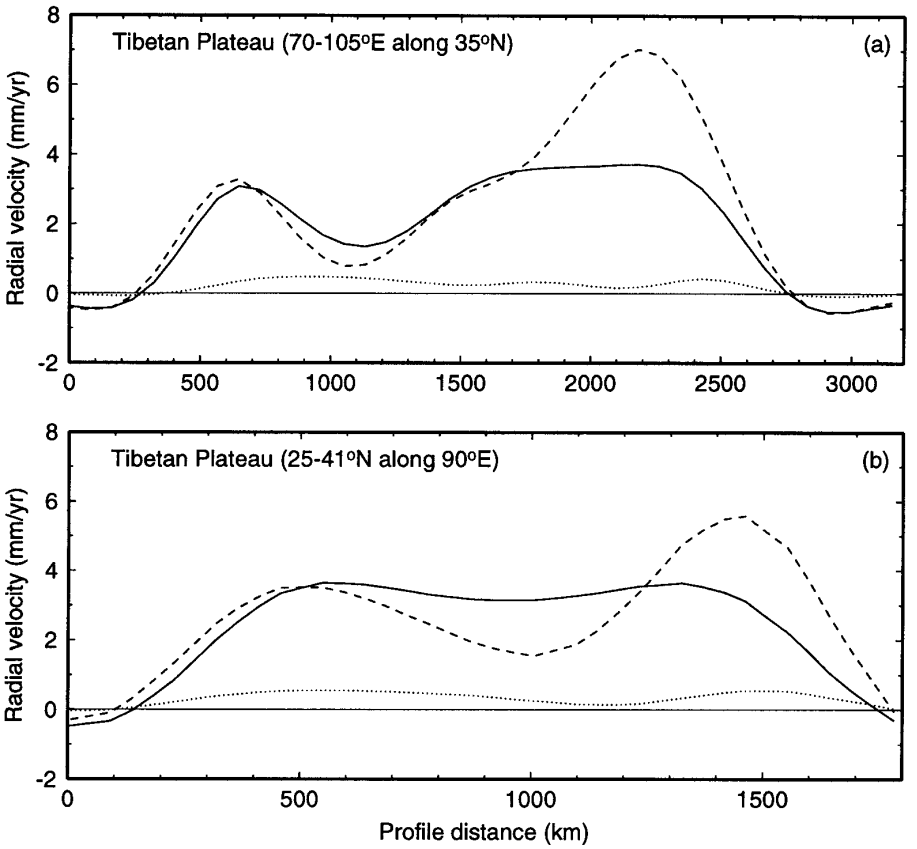

FIG. 7. Profiles of present radial velocities across the Tibetan Plateau for ice models KUHLE (solid lines), DERBY (dotted lines), and TIBET-4 (dashed lines).

KUHLE and TIBET-4, while the contribution arising from the melting of the smaller ice models GUPTA and DERBY is negligible (<1.5 m) compared to the total ESL rise. While the simple linear deglaciation of ice models KUHLE, GUPTA, and DERBY contributes to the ESL until Late Pleistocene times, the meltwater peak released by ice model TIBET-4 is sharper and no significant meltwater runs into Bengal Bay after about 12,000 yr B.P.

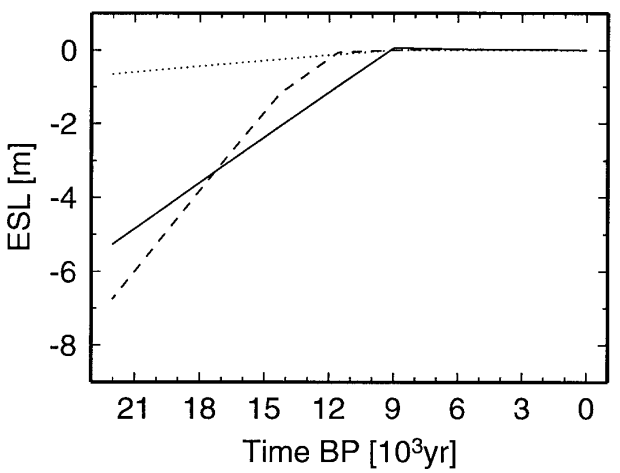

FIG. 8. Eustatic sea level rise related to melting of ice model KUHLE (solid lines), DERBY (dotted lines), and TIBET-4 (dashed lines).

FREE AIR GRAVITY ANOMALY

Undoubtfully the largest contribution to the free-air gravity anomaly (FAGA hereafter) is related to large-scale tectonic processes active in this region, along with the subduction of the Indian plate under the Eurasian plate, resulting in

TABLE 2
Eustatic Sea-Level Rise

Ice model	Sea-level rise [m]
KUHLE	5.2
GUPTA	1.3
DERBY	0.6
TIBET-4	6.6

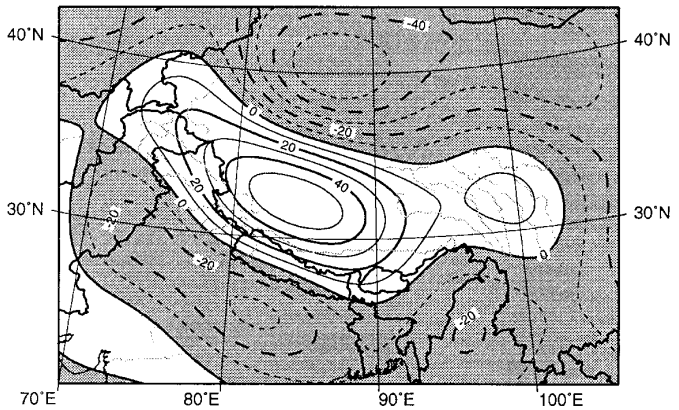

FIG. 9. Observed present free-air gravity anomaly over high Asia derived from gravity model PGS-3520 (Lerch *et al.,* 1979). Contours are drawn every 10 mGal; gray-shaded regions are negative.

large orogenic belts (Himalaya, Karakoram) and the Tibetan Plateau. As expected from the excess masses in the uplifted region (e.g., Lambeck, 1988), the observed FAGA over the entire plateau is positive, with peak values up to +60 mGal over the western part (Fig. 9). On the other hand, a deglaciation of the Tibetan Plateau based on a large Pleistocene ice sheet as proposed by Kuhle *et al.* (1989) with ongoing present uplift will result in a mass deficiency due to the disequilibrium and we therefore expect negative values for the FAGA over the previously glaciated areas. This clearly is not observed in the gravity field, and thus the contribution to the FAGA arising from a glaciation cycle will be only a secondary effect.

The peak values for the predicted FAGA related to the Pleistocene glaciation cycle are summarized in Table 3 for all ice models used in this approach. It is readily seen that significant contributions are predicted only from ice models KUHLE and TIBET-4, with negative peak values around −5.4 mGal; values for both of the other contributions being negligible. The predicted FAGA field for the two ice models KUHLE and TIBET-4 is shown in Figure 10. Again, it can be seen that the minima are correlated with the centers of the formerly glaciated regions, with a broad region of negative values below −4 mGal for the large ice sheet proposed by Kuhle *et al.* (1989) over the entire Tibetan Plateau and more focused regions comprising values below −4 mGal over Quaidam Pendi and the Lhasa region for ice model TIBET-4. Comparing the predicted and the observed FAGA, we conclude that a Late Pleistocene glaciation cycle as proposed by Kuhle *et al.* (1989) would be able to reduce the tectonic part in the observations over the Tibetan Plateau by only about 8%. A similar reduction will arise from ice model TIBET-4. On the other hand, a partial ice cover of the Tibetan Plateau as proposed by Derbyshire *et al.* (1991) as well as a thin ice cover as proposed by Gupta *et al.* (1992b) will have no significant effect on the present perturbation of the gravity field.

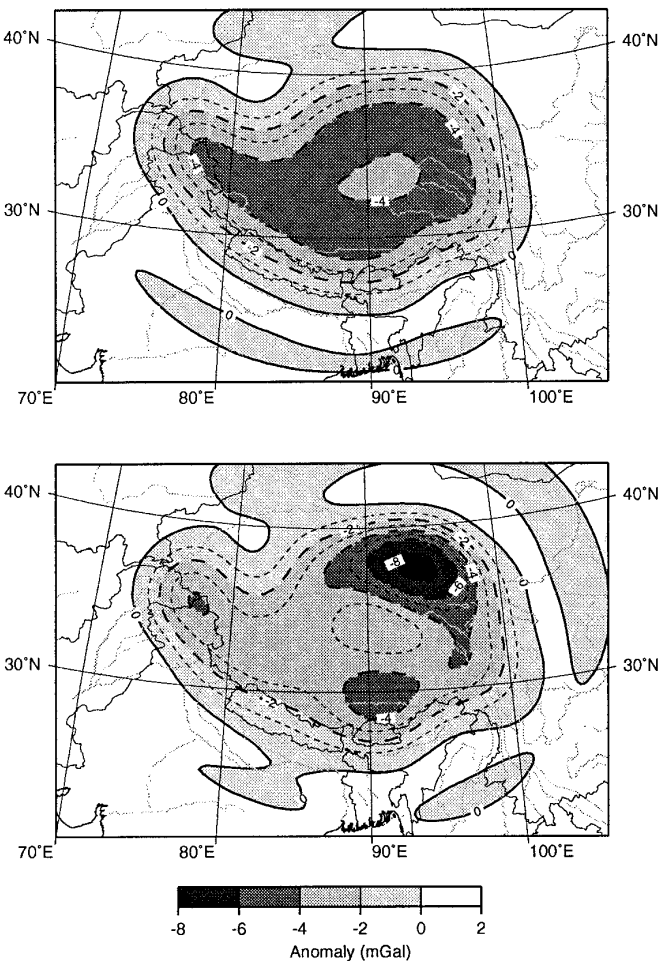

FIG. 10. Predicted present free-air gravity anomaly over high Asia according to ice model KUHLE (top) and TIBET-4 (bottom).

TABLE 3
Maximum Free-Air Gravity Anomalies (FAGA) and Changes (ΔFAGA) Related to Different Ice Models

Ice model	FAGA [mGal]	ΔFAGA [μGal/yr]
KUHLE	−4.7	−0.6
GUPTA	−1.2	−0.2
DERBY	−0.7	−0.1
TIBET-4	−8.6	−1.0

A simple geodetic experiment involving repeated measurements of the gravity along various profiles across the Tibetan Plateau could be used to constrain the rate of change of the gravity field (Table 3). Repeated measurements over three decades in Fennoscandia have reduced the standard

error of the measurements to 0.2 μGal/yr (Ekman and Mäkinen, 1996). For ice models KUHLE and TIBET-4 the annual change in FAGA is approximately 0.6 and 1.0 μGal/yr, thus well above the noise level.

CONCLUDING REMARKS

In this paper we have investigated the effect of a Late Pleistocene glaciation cycle on the Tibetan Plateau on present uplift rates, free-air gravity anomalies, and eustatic sea-level rise. In view of the controversial discussions of the LGM ice cover of the Tibetan Plateau in the literature of the past decade, we have derived lower and upper bounds on the present observable parameters using minimalistic and maximalistic ice models. The range of glacially induced uplift rates and free-air gravity anomalies predicted can be used to determine uncertainties in the nontectonic contribution of the above mentioned observable parameters. We have argued that the glacially induced uplift rate can contribute up to 7 mm/yr of vertical uplift and up to 2 mm/yr horizontal extension over the Tibetan Plateau, if the presence of a large ice sheet during the LGM as proposed by Kuhle *et al.* (1989) is taken into account. This upper bound could explain more than 50% of the observed present uplift rate. The glacially induced free-air gravity anomalies arising from an extensive ice sheet, with peak values around −5.4 mGal, would contribute a reduction of up to 8% of the observed signal attributed to tectonics.

In contrast, a thinner ice cover as proposed by Gupta *et al.* (1992b) or a partial ice cover as proposed by Derbyshire *et al.* (1991) would leave no ''fingerprints'' on the observed present uplift rate or free-air gravity anomalies. In view of the improvements of space–geodetical observations (GPS, gravity field) expected in the near future and with the help of physically consistent modeling of the cooling history of the Himalaya and the Tibetan Plateau, such a discrimination of the tectonic and nontectonic contributions would improve our knowledge of this fascinating region.

ACKNOWLEDGMENTS

We thank Peter Clark and Ed Derbyshire for their constructive reviews of this manuscript. The figures in this paper were drawn using the GMT graphics package (Wessel and Smith, 1991).

REFERENCES

Amano, K., and Taira, A. (1992). Two-phase uplift of Higher Himalayas since 17 ma. *Geology* **20,** 391–394.

Burbank, D. W. (1992). Causes of recent Himalayan uplift deduced from deposited patterns in the Ganges basin. *Nature* **357,** 680–683.

Copeland, P., and Harrison, T. M. (1990). Episodic rapid uplift in the Himalaya revealed by $^{40}Ar/^{39}Ar$ analysis of detrital K-feldspar and muscovite, Bengal fan. *Geology* **18,** 354–357.

Cui, Z. (1964). On the problem of Pleistocene ice cover patterns in west China. *Acta Geographica Sinica* **44,** 2. [In Chinese]

Denton, G. H., and Hughes, T. J. (1981). ''The Last Great Ice Sheets.'' Wiley, New York.

Derbyshire, E., Shi, Y., Li, J., Zheng, B., Li, S., and Wang, J. (1991). Quaternary glaciation of Tibet: the geological evidence. *Quaternary Science Reviews* **10,** 485–510.

Dziewonski, A. M., and Anderson, D. L. (1981). Preliminary reference Earth model. *Physics of the Earth and Planetetary Interiors* **25,** 279–356.

Ekman, M. (1996). A consistent map of the postglacial uplift of Fennoscandia. *Terra Nova* **8,** 158–165.

Ekman, M., and Mäkinen, J. (1996). Recent postglacial rebound, gravity change and mantle flow in Fennoscandia. *Geophysical Journal International* **126,** 229–234.

Fairbanks, R. G. (1989). A 17000-year glacio–eustatic sea-level record: influence of glacial melting rates on the younger Dryas event and deep-ocean circulation. *Nature* **342,** 637–642.

Gupta, S. K., Sharma, P., and Shah, S. K. (1992a). Source of freshwater influx at LGM in the Indian Ocean: an alternative interpretation. *Journal of Quaternary Science* **7,** 247–255.

Gupta, S. K., Sharma, P., and Shah, S. K. (1992b). Constraints on ice sheet thickness over Tibet during the last 40000 years. *Journal of Quaternary Science* **7,**(4), 283–290.

Harrison, T. M., Copeland, P., Kidd, W. S. F., and Yin, A. (1992). Raising Tibet. *Science* **255,** 1663–1670.

Hedin, S. (1922). ''Southern Tibet.'' Genesalstabens Litografiska anstalt, Stockholm.

Huntington, E. (1906). Pangong: A glacial lake in the Tibetan Plateau. *Journal of Geology* **14,** 599–617.

Huybrechts, P. (1992). ''The Antarctic Ice Sheet and Environmental Change: A Three-Dimensional Modelling Study.'' Ber. Polar-forschung 99, Bremerhaven.

Jackson, M., and Bilham, R. (1994). Constraints on Himalayan deformation inferred from vertical velocity fields in Nepal and Tibet. *Journal of Geophysical Research* **99** (B7), 13,897–13,912.

Johnston, P. (1993). The effect of spatially non-uniform water loads on prediction of sea-level change. *Geophysical Journal International* **114,** 615–634.

Kaufmann, G. (1997). The onset of Pleistocene glaciation in the Barents Sea: implications for glacial isostatic adjustment. *Geophysical Journal International* **131,** 281–292.

Kuhle, M. (1988a). Zur Auslöserrolle Tibets bei der Entstehung der Eiszeiten. *Spektrum der Wissenschaft* **1,** 16–20.

Kuhle, M. (1988b). The Pleistocene glaciation of Tibet and the onset of ice ages: an autocycle hypothesis. *GeoJournal* **17** (4), 581–595.

Kuhle, M. (1988c). Geomorphological findings on the build-up of Pleistocene glaciation in southern Tibet and on the problem of inland ice; results of the Shisha Pangma and Mt. Everest Expedition 1984. *GeoJournal* **17** (4), 457–511.

Kuhle, M., Herterich, K., and Calov, R. (1989). On the ice age glaciation of the Tibetan Highlands and its transformation into a 3-D model. *GeoJournal* **19** (2), 201–206.

Lambeck, K. (1988). ''Geophysical Geodesy. The Slow Deformations of the Earth.'' Oxford Univ. Press, Oxford.

Lambeck, K. (1996). Limits on the areal extent of the Barents Sea ice sheet in Late Weichselian time. *Global and Planetary Change* **12,** 41–51.

Lambeck, K., Johnston, P., and Nakada, M. (1990). Holocene glacial rebound and sea-level change in NW Europe. *Geophysical Journal International* **103,** 451–468.

Lambeck, K., Johnston, P., Smither, C., and Nakada, M. (1996). Glacial rebound of the British Isles: III. Constraints on mantle viscosity. *Geophysical Journal International* **125,** 340–354.

Lerch, F. S., Klosko, S. M., Laubscher, R. E., and Wagner, C. A. (1979). Gravity model improvement using GEOS 3 (GEM 9 and GEM 10). *Journal of Geophysical Research* **84,** 3897–3916.

Longman, I. M. (1962). A Green's function for determining the deformation of the Earth under surface mass loads. *Journal of Geophysical Research* **67** (2), 845–850.

Love, A. E. H. (1911). ''Some Problems of Geodynamics.'' Cambridge Univ. Press, Cambridge, UK.

Luo, L., and Yang, Y. (1963). Analysis of geomorphological development in Western Sichuan and Northern Yunan. *In* ''Geographical Essay,'' Vol. 5. Science Press, Beijing. [In Chinese]

Mitrovica, J. X. (1996). Haskell [1935] revisited. *Journal of Geophysical Research* **101** (B1), 555–569.

Mitrovica, J. X., and Davis, J. L. (1995). The influence of a finite glaciation phase on predictions of post-glacial isostatic adjustment. *Earth and Planetary Science Letters* **136,** 343–361.

Mitrovica, J. X., and Peltier, W. R. (1989). Pleistocene deglaciation and the global gravity field. *Journal of Geophysical Research* **94,** 13,651–13,671.

Mitrovica, J. X., Davis, J. L., and Shapiro, I. I. (1994). A spectral formalism for computing three-dimensional deformations due to surface loads 1. Theory. *Journal of Geophysical Research* **99** (B4), 7057–7073.

Molnar, P. (1987). Inversion profiles of uplift rates for the geometry of dip-slip faults at depth, with examples from the Alps and the Himalayas. *Annales Geophysicae* **5,** 663–670.

Molnar, P., and England, P. (1990). Late Cenozoic uplift of mountain ranges and global climate change: chicken or egg? *Nature* **346,** 29–34.

Nakada, M., and Lambeck, K. (1987). Glacial rebound and relative sea-level variations: a new appraisal. *Geophysical Journal of the Royal Astronomical Society* **90,** 171–224.

Nakada, M., and Lambeck, K. (1988). The melting history of the late Pleistocene Antarctic ice sheet. *Nature* **333,** 36–40.

Peltier, W. R. (1974). The impulse response of a Maxwell Earth. *Reviews of Geophysics and Space Science* **12** (4), 649–669.

Peltier, W. R. (1994). Ice age paleotopography. *Science* **265,** 195–201.

Richards, M. A., and Hager, B. H. (1984). Geoid anomalies in a dynamic Earth. *Journal of Geophysical Research* **89,** 5987–6002.

Rind, D., and Peteet, D. (1985). Terrestrial conditions in the last glacial maximum and CLIMAP sea surface temperature estimates: Are they consistent: *Quaternary Research* **24,** 1–22.

Rutter, N. (1995). Problematic ice sheets. *Quaternary International* **28,** 19–37.

Schneider, H.-J. (1957). Tektonik and Magmatismus im NW-Karakorum. *Geologische Rundschau* **46,** 426–476.

Shi, Y. (1992). Glaciers and glacial geomorphology in China. *Zeitschift für Geomosphologie N. F.* **86,** 51–63.

Shi, Y., Ren, B., Wang, J., and Derbyshire, E. (1986). Quaternary glaciation in China. *Quaternary Science Reviews* **5,** 503–507.

Sinitzin, V. M. (1958). ''Central Asia.'' Central Publishing House, Moscow.

Sun, D., and Wu, X. (1986). Preliminary study of Quaternary tectonoclimatic cycles in China. *Quaternary Science Reviews* **5,** 497–501.

Tafel, A. (1908). Vorläufiger Bericht über eine Studienreise in Nord-West-China and Ost-Tibet. *Zeitschrift für GEB,* 377–395.

Trinkler, E. (1930). Ice age on the Tibetan Plateau and in the adjacent region. *Geographical Journal* **75,** 225–232.

Tushingham, A. M., and Peltier, W. R. (1991). Ice-3G: a new global model of late Pleistocene deglaciation based upon geophysical predictions of post-glacial relative sea level change. *Journal of Geophysical Research* **96,** 4497–4523.

von Wissmann, H. (1959). Heutige Vergletscherung und Schneegrenze in Hochasien. *Akademie der Wissenschaften und der Literatur in Mainz, Mathematisch-Naturwissenschaftliche Klasse, Abhandlungen* **11,** 1103–1407.

Wang, M., and Zheng, M. (1965). Remnants of quaternary glaciation on the Tibetan Plateau. *Acta Geographica Sinica* **31,** 63–72. [In Chinese]

Ward, F. K. (1934). The Himalaya east of the Tsangpo. *Geographical Journal* **84,** 369–397.

Wessel, P., and Smith, W. H. F. (1991). Free software helps map and display data. *EOS* **72,** 441–446.

Zeitler, P. K. (1985). Cooling history of the NW Himalaya, Pakistan. *Tectonics* **4,** 127–151.

Zheng, B. (1989). Controversy regarding the existence of a large ice sheet on the Qinghai–Xizang (Tibetan) Plateau during the Quaternary period. *Quaternary Research* **32,** 121–123.

Zheng, B., and Li, J. (1981). Quaternary glaciation of the Qinghai–Xizang Plateau. *In* ''Geological and Ecological Studies of Qinghai-Xizang Plateau,'' pp. 1631–1640. Science Press, Bejing.